International Journal of Hydrogen Energy 71 (2024) 1056–1069

Contents lists available at ScienceDirect

International Journal of Hydrogen Energy

journal homepage: www.elsevier.com/locate/he

Transforming abandoned petroleum wells in the Nigerian sector of the Chad basin into triplet borehole heat exchangers for sustainable power generation

Abubakar Magaji [a], Bin Dou [a,*], Gianluca Gola [b], Sani Ali [c], Ibrahim AL-Wesabi [d]

[a] Faculty of Engineering, China University of Geosciences, Wuhan, 430074, China
[b] Institute of Geosciences and Earth Resources, National Research Council, Via Valperga Caluso, 35, 10125, Torino, Italy
[c] School of Science, Abubakar Tafawa Balewa University Bauchi, Nigeria
[d] School of Automation, China University of Geosciences, Wuhan, 430074, China

ARTICLE INFO

Handling Editor: Dr Z Sun

Keywords:
Deep closed-loop system
Geothermal energy
Triplet borehole heat exchanger
Sustainability
Numerical simulation

ABSTRACT

This study pioneers a transformative approach to sustainable energy recovery, repurposing abandoned petroleum wells in the Nigerian Chad Basin as a triplet-deep closed-loop heat exchanger. We employed a computational numerical approach to designed two deep closed loop systems, which share a common production well, and to evaluate the thermal performance as well as its sustainability over a period of 25 years. The geometrical configuration consists of two injection wells, which converge to the common production one doubling the flow rate at surface and minimising the heat loss during the ascent of the fluid. The availability of detailed abandoned well specifications enabled us to constrain three-dimensional geological and thermal models of the undisturbed underground and, subsequently, to simulate numerically the production temperature and the thermal disturbance in the surrounding rocks. A comprehensive sensitivity analysis optimized the best operational design for total recovered thermal energy and uninterrupted heat recovery. When the deep close loop heat system operates with a fluid circulation rate of 0.03 m^3s^{-1} and an injection temperature of 20 °C, it sustains a production temperature of over 100 °C, which generates total recovered thermal energy of 9730 TW_{th} and 817 TW_e over 25 years (9000 days). The average annual thermal and electricity productions of 389 TW_{th} and 33 TW_e, respectively, are more than the demand of the entire population of Magumeri district. The study's findings offer practical implications for policymakers, industry stakeholders, and local communities, emphasising the potential for socio-economic development while fostering environmental stewardship in the Nigerian Chad Basin.

1. Introduction

The growing need for sustainable, low-emission energy sources has made geothermal power a viable substitute. Geothermal energy is continuously available, and unlike other renewable energy sources like solar and wind, it can be used to provide a consistent supply of energy when needed. The worldwide energy transition to more renewable and sustainable sources can be greatly aided by geothermal energy [1]. In order to benefit from geothermal energy, which produces electricity from the heat of the earth, numerous technologies were created [2,3]. The International Energy Agency (IEA) projected that by 2023, installed geothermal power capacity worldwide will increase from 7 GW in 1995 to over 17 GW [4]. However, the high expense of drilling for geothermal projects prevents this technology from being widely used [5,6]. Approximately half of the total expenses in a geothermal project can be attributed to drilling costs [7]. Only approximately 1% of the world's geothermal resources are exploited [8].

Across the globe, there are an estimated 20 to 30 million abandoned petroleum wells [9]. These wells typically reach considerable depths, ranging from 1000 m to over 3000 m below ground level [10–12]. Moreover, most of these wells exhibit bottom temperatures often exceeding 100 °C [11,13]. According to the Ministry of Petroleum Resources, Nigeria has159 operational oil fields, with 1481 active petroleum wells [14], most of these wells are in operation for over 50 years, this clearly shows they already reached their potentials, are on the declining stage. Therefore, it is evident that the surplus abandoned gas

* Corresponding author.
E-mail addresses: abubakarmagaji51@gmail.com (A. Magaji), doubin@cug.edu.cn (B. Dou), g.gola@igg.cnr.it (G. Gola), alisani2000@yahoo.co.uk (S. Ali), ibrahimxiao@gmail.com (I. AL-Wesabi).

https://doi.org/10.1016/j.ijhydene.2024.05.275
Received 13 March 2024; Received in revised form 29 April 2024; Accepted 17 May 2024

and oil wells needs to be managed [15]. These abandoned wells can still yield geothermal energy by creating or enhancing geothermal system [16,17]. One potential remedy for the previously mentioned issue is to repurpose abandoned oil and gas wells for the production of geothermal power and heating/cooling. Through that, the cost of drilling for geothermal projects would be reduced, and the usefulness of abandoned wells would be increased [6].

Researchers are currently exploring the potential of repurposing abandoned petroleum wells to extract geothermal energy to mitigate drilling costs. The heat extraction performance of deep geothermal development has been extensively studied in the past using variety of techniques. Transforming these abandoned wells into deep borehole heat exchangers (DBHEs) enables the extraction of geothermal energy [18–20]. A DBHE is a closed-loop system that involves the installation of pipes in deep wells for efficient heat exchange [21–23]. A deep borehole heat exchanger (DBHE) serves dual purpose by actively preventing potential leakages of greenhouse gases and water contamination from abandoned wells [24,25]. Experimental and numerical investigations of this concept were conducted by Kohl et al., 2000 [26]; Kohl et al., 2002 [27] employed a coaxial system in which the production and injection wells are located within a single borehole where fluid descends through the pipe's centre and rises again, this method became an unorthodox means of harnessing geothermal energy and overcoming the usual limitations of hydrothermal systems. In the Western Canadian sedimentary Basin near Hinton, Hu et al., 2021 [28] examined the viability of extracting geothermal energy from abandoned petroleum wells, and they discovered that the doublet well system outperformed the single well system. Using multilateral wells to connect two or more wells, underground heat exchangers sub-horizontally can be created from underutilised or abandoned wells [29,30]. Zhao et al., 2020 [31] presented a thorough heat extraction and recovery temperature curve for a three-year short period of operation from abandoned wells. Henrik et al., 2016 [32] conducted experiments to confirm the efficacy of their transient numerical model for coaxial borehole heat exchangers.

In Kiskunhalas, Hungary, Mining Support Ltd. Installed the first operational DBHE system, turning an abandoned oil well into a geothermal one [33,34]. The primary disadvantage of DBHE is its low heat recovery efficiency compared to conventional geothermal plants. There is still requirement for additional technological advancements and research to put the borehole design into practice [35–37].

This innovative approach addresses energy challenges and presents a scalable model for sustainable development. By harnessing abundant geothermal resources and repurposing existing infrastructure, the proposed two deep closed-loop heat exchanger (DCHE) system is a promising solution for regions with abandoned petroleum wells, contributing to the global transition towards clean and renewable energy sources. Widespread application will increase the use of geothermal energy, raising its percentage in Africa's overall energy production and helping to achieve the seventh Sustainable Development Goal of the United Nations by 2050.

2. Data and methods

2.1. Geological and geothermal setting of Bornu Basin

North-eastern Nigeria's Bornu Basin is a portion of the Chad Basin that has not yet been thoroughly investigated for hydrocarbons [38]. Several authors have reported on the stratigraphy of the Bornu-Chad basin [38–41]. The Chad Basin has an average geothermal heat flow of 81 mWm^{-2}, ranging from 75 to 125 mWm^{-2} [42]. The basin heat flow is greater than the world average of 65 mWm^{-2} in continental crust [43], with an average surface temperature of 27 °C [44,45].

The hydrocarbon exploration of the Chad Basin (Bornu) in Nigeria was carried out by the Nigerian National Petroleum Investment Management Services (NAPIMS) of the Nigerian National Petroleum Corporation (NNPC), with approximately 23 wells drilled in the Bornu region of the Chad Basin, with depth ranges from 1500 m to 4600 m [46,47]. The well-log data used in this study were obtained as part of the Chad Basin petroleum exploration drilling program. Data collected are from log headers of the drilled wells, including the lithostratigraphic information and the bottom hole temperatures recorded at each logging run. In our research, we selected Gubio (GUB), Ngor (NGO), and Ngamma (NGA) hydrocarbon exploratory wells with true vertical depths of 3637 m, 3686 m, and 3254 m below the ground level, respectively. The wells explored a thick Albian to recent sedimentary sequence, which lies unconformably on the Precambrian basement. The deposition took place under varying conditions with each deposit representing one complete cycle of transgression and regression. The oldest Bima Fm. consist of continental, coarse to medium grained sandstones intercalated with carbonaceous clays, shales, and mudstones. The Turonian Gongila Fm. comprises calcareous shales, silty sandstones, and sandstones, which conformably overlies the Bima Fm. and represents a transitional sequence to the overlying marine Fika Fm represented by open marine shales with intercalation of limestones. The transitional Gombe Fm. rests unconformably on the Fika Fm. and comprises siltstones, sandstones, and claystone deposited during the Maastrichtian uplift episode. The continental Kerri-Kerri Fm. of Palaeocene age and the Chad Fm. of Pleistocene age are the younger stratigraphic units made-up of fine to coarse sand and clays [48–50]. The detailed lithostratigraphic information from the GUB, NGO, and NGA deep exploratory wells together with the estimated thermal properties are presented in Table 1. Due to the proximity to the wells, Magumeri district is selected as pilot-site to evaluate the energy and heat demand to be supplied by the DCHE system. In Fig. 1 the actual position of the wells and the selected district are displayed.

2.2. The numerical model

2.2.1. Geometrical configuration of DCHE

To extract geothermal energy, a cold primary fluid is injected into the two injection wells at a constant flow rate. As the fluid flows along the vertical and horizontal sections, it undergoes heating by conduction from the surrounding rock. In the final stage, the fluid ascends back to the surface through the production well. Fig. 2 shows the intended layout of the DCHE, which comprises three vertical boreholes, two injections, and one production. An efficient two-closed-loop system is created by connecting these wells with an insulated pipeline at the surface and a horizontal section at depth. A heat-releasing exchanger at the geothermal plant circulates a primary fluid in a closed-loop system. The deviated drilling sections begins at the end of the vertical injection wells H. The deviation follows a smoothly curved path with tangents of specified length of 250 m. The drilling progresses along this tangent with a consistent radius until 45° inclination is achieved. At that point, it resumes at a 90° entry angle using the same build rate as before, yielding a final horizontal offset K. The production well has a vertical height M, with a 90^{o} entry angle. The length's horizontal section, L, is the last section to be drilled, and it is through this section that the wells are connected horizontally (see Fig. 3).

To examine the DCHE systems' heat performance, we reconstructed the actual borehole locations of GUB, NGO, and NGA boreholes using the exact coordinates data. The DCHE of our simulation study comprises two loop systems. Loop one, NGO and NGA, has a total length of 12500 m, while loop two includes NGA and GUB, which have a full length of 12700 m. The three vertical sections of our simulation boreholes are 4000 m each, the horizontal distance between NGO and NGA is 4500 m and 4700 m from NGA to GUB. We planned the veered section's drilling at a TVD of −4000 m above sea level, attaining a degree (90^{o}) entry angle. In our simulation, we designed GUB and NGO to be the injection wells while NGA to be the production well.

Presently, the greatest recorded subsurface depth within a borehole is 6062 m, achieved in an oil well situated within the Villafortuna-Trecate Field in Italy, and the utmost extent of lateral branch length

Table 1
Generalised stratigraphy and thermal properties of Ngor (NGO), Gubio (GUB), and Ngamma (NGA) abandoned wells. Thermal conductivity (λ), heat capacity (Cρ) density (ρ), and depths of each formation [51,46].

Formation	Materials	Age	λ ($Wm^{-1}K^{-1}$)	ρ (kgm^{-3})	Cρ J/ (kg·K)	TVD (m a.s.l.)		
						NGO	GUB	NGA
Cd	clays with sand and interbeds	Holocene/Pleistocene	3.403	2025	1120	355	391	366
Kk	Iron-rich sandstones and clay covered by plaint of laterite	Miocene/Pliocene	3.592	2038	1130	−646	−724	−640
Gm	Sandstone, siltstone, and clay with coal beds	Maastrichtian	2.991	2638	872	−1322	−1580	−1286
Fk	Shale, dark Grey to black, gypsiferous with limestone beds	Campanian/Santonian Coniacian	3.042	2431	947	−1845	−2139	−1913
Gl	Alternating sandstone and shale with limestone beds	Senonian/Turonian	3.012	2455	947	−2624	−2843	−2655
Bm	Sandstone, gravely to medium-grained, poorly sorted, and highly felspathic	Turonian/Albian/Aptian	3.212	2515	915	−3686	−3637	−3254

Note: Cd – Chad: Kk - Kerri Kerri: Gm – Gombe: Fk – Fika: Gl – Gongila: Bm - Bima.

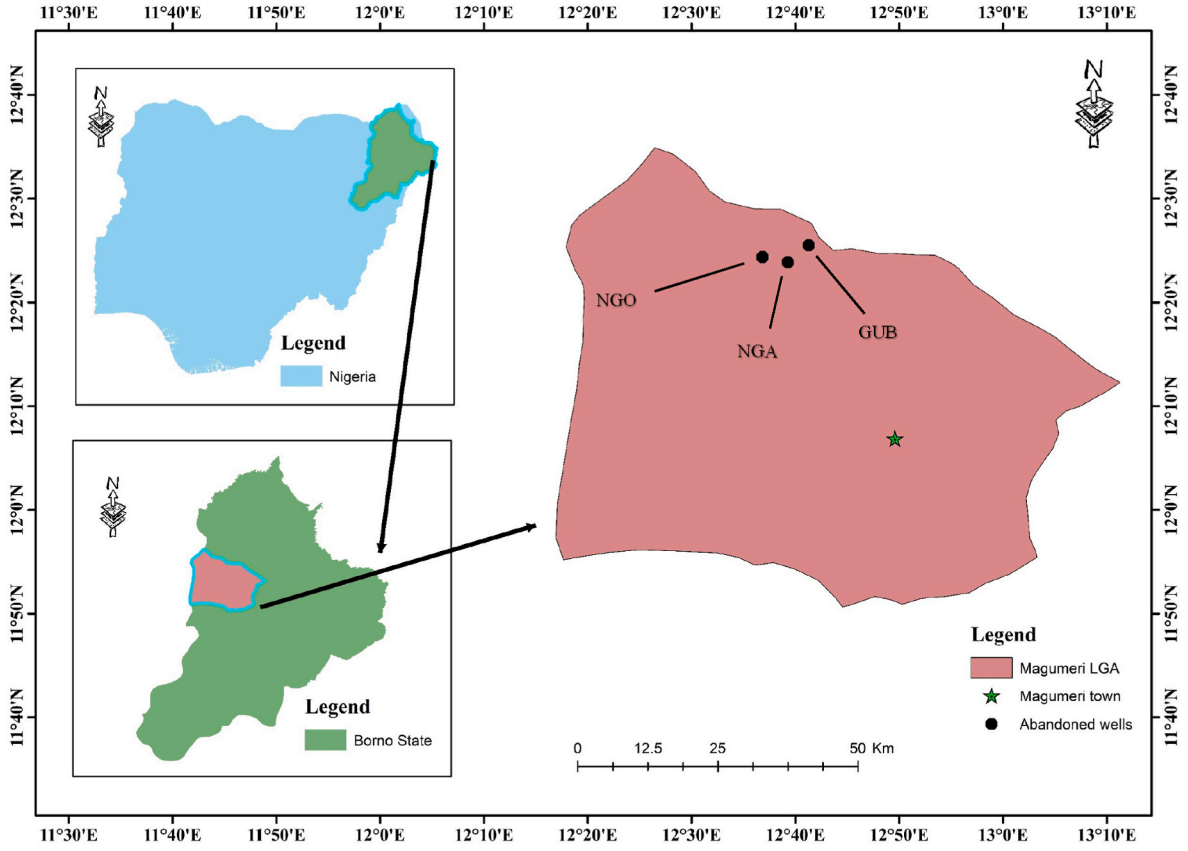

Fig. 1. Study area map with deep abandoned petroleum wells (black circles).

observed is 15,000 m in the O-14 well within the Chayvo field, located offshore Sakhalin, Russia [28].

Globally, diverse geothermal conversion technologies are implemented, with each approach customized to suit the specific characteristics of the available resources [52]. Despite the intermediate temperature gradient examined in this study, it is assumed that the generated electrical power will be produced under long-term conditions, with the water in the DCHE remaining in a state of pure liquid below its saturation point. Therefore, binary system is adopted as the method to convert thermal energy into electrical energy. The binary cycle geothermal power plants, utilising a secondary circulation system with an alternative working fluid featuring lower evaporating conditions than the geothermal fluids. Fig. 2e illustrates binary power plant designed for converting the thermal energy extracted by the DCHE into electrical power.

2.2.2. Mathematical formulation

When constructing the DCHE numerical model, both the geological and thermal information from the available boreholes is considered. formations and the borehole, are considered as the two main mechanisms for heat transfer, thermal conduction and advection. Zero velocity components are assured about the borehole axis by maintaining a large diameter-to-length ratio. This provision facilitates the full development of fluid flow within the two closed-loop systems.

The temperature of the surrounding rocks rises with depth, which results in heat exchange between a Newtonian fluid that circulates within the two closed loops. The numerical computation solves the fluid's 1D temperature, pressure, and velocity. Using Newton's cooling law, heat transfer is described as pure conduction on the wall-fluid interface. We used the IAPWS-IF97 formulation to define the thermodynamic properties of freshwater, assuming it to be the primary fluid [34,52]. The fluid's mass and momentum conservation equations are as follows.

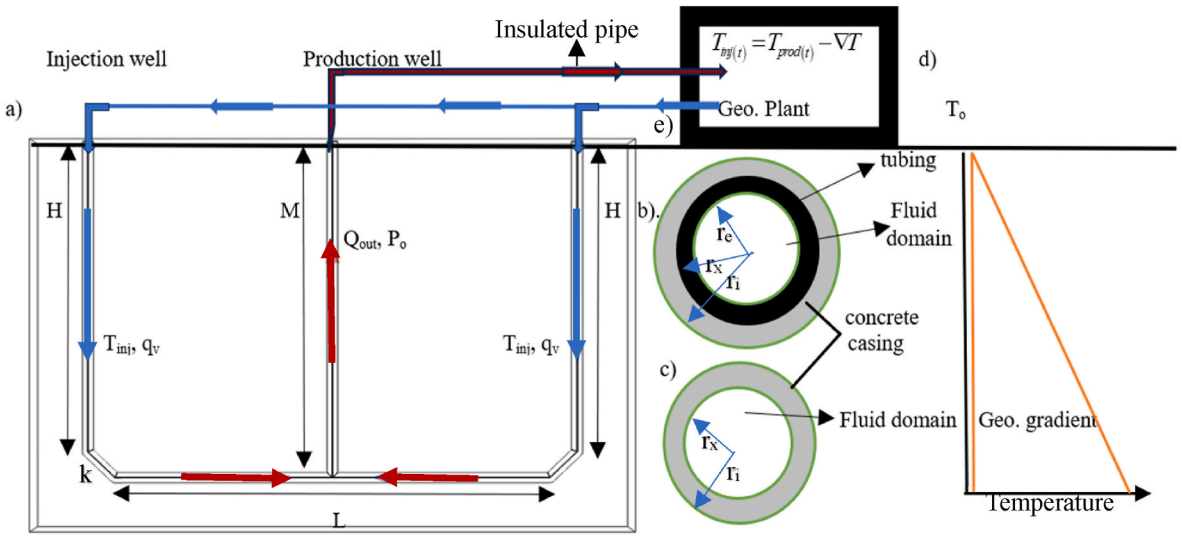

Fig. 2. The two-deep closed-loop heat exchanger's schematic setting and numerical boundary conditions are shown in (a); cross-sectional profiles of the borehole (b) concrete casing (c); Unaltered subterranean geothermal environment (d); geothermal conversion plant (e). ri is the outer radius of the concrete casing, rx is the outer radius of the tubing, and re is the inner radius of the borehole.

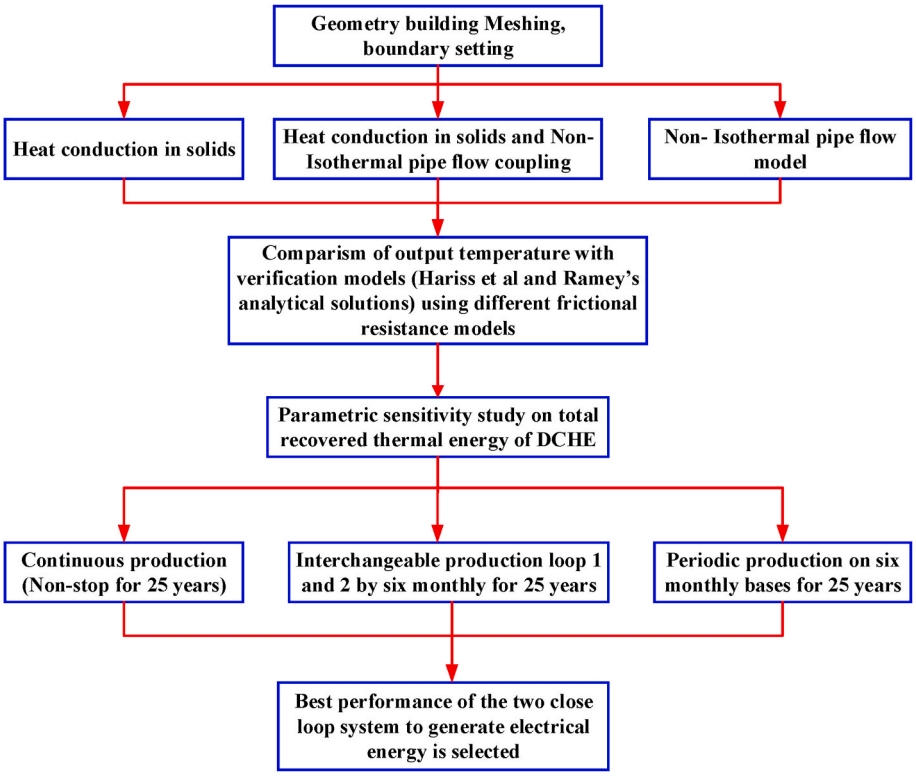

Fig. 3. Flowchart depicting the numerical modelling process for doublet deep Borehole Heat Exchangers (DCHEs).

$$\rho_m \frac{\partial u}{\partial t} + \rho_m u.\nabla u = \nabla p - f_D \frac{\rho_m}{2D} u|u| + \mathscr{F} \quad (1)$$

$$\frac{\partial A\rho_m}{\partial t} + \nabla \cdot (A\rho_m u) = 0 \quad (2)$$

Where ρ_m (kg m^{-3}) is the fluid density, u (ms^{-1}) the tangential, cross-section averaged, fluid velocity, t (s) the time, p (Pa) the pressure, F (Nm^{-3}) the gravitational volume force, D (m) and A (m^2) the borehole inner diameter and the cross-section area, respectively, and f_D the dimensionless Darcy-Weisbach (D-W) frictional factor. The Stokes model [53] was adopted to account for the pressure drop caused by viscous shear along the wellbore. The D-W friction factor can be solved as:

$$f_D = \frac{64}{\mathrm{Re}} \quad (3)$$

$$\mathrm{Re} = \frac{\rho u D}{\mu} \quad (4)$$

With Re (dimensionless) the Reynold number and μ (Pa s) the fluid

dynamic viscosity.

The borehole and surrounding rock energy conservation equations are, respectively:

$$A(\rho c_p)_m \frac{\partial T_m}{\partial t} + A(\rho c_p)_m u \cdot \nabla T_m = \nabla \cdot A\lambda_m \nabla T_m + f_D \frac{A\rho_m}{2D}|u|^3 + Q_w \quad (5)$$

$$(\rho c_p)_n \frac{\partial T_n}{\partial t} = \nabla \cdot \lambda_n \nabla T_n + Q_w \quad (6)$$

where λ represents the thermal conductivity ($Wm^{-1}K^{-1}$), T the absolute temperature (K), and ρc the volumetric heat capacity ($J\ m^{-3}\ K^{-1}$). The fluid and rock are denoted by the subscripts m and n, respectively. In Eq. (5), the second term on the right represents the heat released in the primary fluid due to internal friction. Eqs. (5) and (6) are coupled by the heat source term, Q_w ($W\ m^{-1}$), which takes into consideration the heat exchange occurring radially between the fluid and the nearby rocks at the interface of the wall and the fluid. The radial transfer of heat is provided by:

$$Q_w = 2\pi h \cdot D(T_n - T_m) \quad (7)$$

where the heat transfer coefficient, h ($Wm^{-2}K^{-1}$), is determined by the inner borehole diameter D, the thermal conductivity of the borehole material (λ_b), the fluid's physical characteristics, and the type of flow, as indicated by Nusselt number (*Nu*):

$$h = Nu\frac{k}{D} \quad (8)$$

With *Nu* the turbulent flow number inside circular pipes [54]:

$$Nu = \frac{(f_D/8)(\mathrm{Re} - 1000)\mathrm{Pr}}{1 + 12.7(f_D/8)^{1/2}(\mathrm{Pr}^{2/3} - 1)} \quad (9)$$

where $\mathrm{Pr} = (cp\ \mu)m/\lambda_m$ is the Prandtl number. For $0.5 \le \mathrm{Pr} \le 2000$ and $3000 \le \mathrm{Re} \le 5{\cdot}10^6$, Eq. (9) is applicable.

The borehole thermal conductivity (λ_b) is evaluated as the weighted sum of the thermal resistances' crossway the borehole accounting for a multiple cylinder-shaped shell with varying thicknesses, as shown in Fig. 2b. Neglecting the thermal diffusivity of the borehole's components is not suitable for simulation on shorter timescales (e.g. hourly). In this work, the 3D numerical model has been applied to investigate the three-dimensional characteristics of heat transfer in and around a deep closed-loop heat exchanger at long time scales (daily to several years). As this temporal constrains, we assumed a quasi-static heat transfer across any shell from the inner bulk to the external rocks.

2.2.3. Numerical boundary condition solver

Equations 1-2 and 5-6 govern the conductive and advective heat transfer process and they were implemented and solved numerically using Comsol Multiphysics software's finite element method. The MUMPS solver was used to solve linear equations [55]. Concerning the borehole boundary conditions at the injection wellhead, a circulation volumetric flow rate (qv, m^3s^{-1}), and a fluid injection temperature (T_{inj}, K) were fixed. Open boundaries at the production well were established. These latter constraints are the wellhead pressure (po, bar) and heat flow (Q_{out}, Wm^{-2}), which offer appropriate boundary conditions at the outlet for problems with mass transfer and convection-dominated heat problems. In the event of high outflow temperatures, a boundary condition pressure po > 1 bar stopped the phase change of the fluid. The production wellhead output (T_{prod}, K) and the heat exchanger's heat-extraction capacity (ΔT, K) are the main factors determining whether the injection temperature was constant or varied over time.

$$T_{inj}(t) = T_{prod}(t) - \nabla T \quad (10)$$

Concerning Yildirim et al., 2010 [56], Eq. (10) disregards the heat losses that occur when fluid is transferred via a superficially insulated pipe that connects the geothermal plant with the injection boreholes. In the surrounding rocks, thermally insulated lateral boundaries were established beyond the DCHE influence radius. The bottom and top boundary conditions consist in fixed temperatures, where the upper thermal boundary corresponds to the mean annual air temperature (T_o, K). We initialised the fluid flow model by setting the velocity and pressure profiles resulting from the steady-state solution. The initial thermal conditions consisted of an isothermal profile of the fluid ($T_z = T_o$) and the conductive steady-state temperature field of the rocks surrounding the closed-loop system.

2.2.4. Analytical modeling

In this study, the fluid's temperature distribution inside the wellbore is modelled analytically as an additional method. The suggested DCHE system's validity was assessed using an analytical formula created by Ramey Jr. In 1962 [57]. Ramey's equation is a commonly adopted method for describing the wellbore temperature distribution [58]. Assuming a single-phase flow inside the well, earlier studies employed Ramey's equation to calculate the temperature distribution in a wellbore fluid as a function of wellbore depth and geothermal gradient [12,59].

$$T(z,t) = az + b - aY + (T_{inj} - b + aY)e^{-Z/Y} \quad (11)$$

Where z is the fluid depth in the wellbore, measured in meters (m); T_{inj} is the injection temperature, measured in °C, b is the surface temperature, measured in °C, and T(z,t) is the fluid temperature in the wellbore. Y is expressed as [59].

$$Y = \frac{q_v C \rho_n f_{(t)}}{2\pi\lambda_m} \quad (12)$$

where λ_m is the thermal conductive coefficient of the surrounding rock, expressed as W/(mK); q_v is the volumetric flow rate, expressed in (m^3s^{-1}), and $f_{(t)}$ is a dimensionless time function that illustrates the transient heat transfer to the formation, which is described by Ref. [59] as.

$$f_{(t)} = -In\left(\frac{rw}{2\sqrt{at}}\right) - 0.29 \quad (13)$$

Where α is the rock's thermal diffusivity, measured in m^2s^{-1}, and rw is the well's radius, measured in (m).

2.3. Production of thermal and electrical energy

Using the numerical models to calculate the temperature variations in production over time, the thermal power was evaluated (G_{th}, MW_{th}), which is defined as:

$$G_{th} = q_v(\rho c_p)_m \cdot (T_{prod} - T_{inj}) \quad (14)$$

The temperatures of production and injection (K) of DCHE are represented by T_{inj} and T_{prod}, respectively. Additionally, we used modern technologies to convert the recovered thermal energy, but only when the temperature reaches 100 °C or above, to produce electrical power. It is recommended to use geothermal binary plants for the production of electricity when the primary fluid temperature is between 120 and 150° Celsius [60], Though an operating binary plant can have a lowest primary fluid temperature of 73° Celsius (that has 306 kJ kg^{-1}enthalpy) as demonstrated from Alaska Chena Spring field [61]. In binary power plants, heat is exchange between the fluid (primary and the working fluid), which boils at lower temperature using heat exchangers [61,62], these closed cycles operate this way. After that, the turbine produces power using the vaporised working fluid. Eq. (15) describes the ideal thermal performance of the triangular cycles [63].

$$\eta_{ideal} = \frac{T_{INLET} - T_{OUTLET}}{T_{INLET} + T_{OUTLET}} \quad (15)$$

The absolute heat exchanger's primary fluid temperatures (K) of the power plant are denoted by T_{INLET} and T_{OUTLET}. It should be noted that the DCHE production temperature (T_{prod}) and the DCHE injection temperature (T_{inj}), assuming no waste of heat, correspond to the heat exchanger temperature inlet (T_{INLET}) and outlet temperature (T_{OUTLET}), respectively. Relative efficiency (ηrel) was introduced to allow for a more practical production of electric power (G_e, MW_e) from thermal energy, as a binary power plant's actual efficiency can only come close to the ideal value. This becomes:

$$G_e = G_{th} \cdot \eta_{ideal} \cdot \eta_{rel} \tag{16}$$

where the upper and lower bounds of ηrel, the relative binary plant performance, are 85% and 44%, respectively, with an average value of 58 ± 4% [63]. On the other hand, a recent global evaluation of the efficiency of real geothermal power plants [61], comprising 31 geothermal binary plants running between 73 and 253° Celsius, the production of electricity is calculated as follows:

$$G_e = G_{th} \cdot [6.9681 \times In(T_{INLET}) - 29.713] \tag{17}$$

or

$$G_e = G_{th} \cdot [6.9681 \times In(h_{INLET}) - 37.929] \tag{18}$$

where enthalpy (kJ kg^{-1}) and temperature degree centigrade of the primary fluid inlet are represented by h_{INLET} and T_{INLET} respectively.

The production of electric power was estimated using Eqs. (16)–(18), considering the power plants' operational capacity is influenced by their design, there is a need for a thorough analysis of the conditions present on-site. These formulas produced similar estimates. For instance, using Eq. (16) and assuming a 58% relative efficiency, the power productions measured with a 70 °C as the outlet temperature, 90 kgs^{-1} as the mass flow rate, and 100 °C temperature or 422 kJ kg^{-1} enthalpy as the minimum and 180 °C temperature, or 794 kJ kg^{-1} enthalpy as the maximum resource temperature, the corresponding values were 0.28 MWe and 3.52 MWe. Utilising Eqs. (17) and (18), somewhat more cautious approximations were computed, which, for the lowest resource temperature, equal 0.27 MW (MWe), and 0.28 MW (MWe), and for the highest resource temperature, 2.83 MW (MWe) and 2.93 MW (MWe), respectively [33].

3. Model validation

Following Gola et al., 2022 [33], we validated our numerical solutions against the analytical solution of Ramey 1962 and the simulated production temperatures by Harris et al., 2021 [6]. In order to perform the code-to-code validation, we used the same input parameters as in Harris et al., 2021 [6] corresponding to a mass flow rate 9 kg s^{-1}, horizontal length 4800 m, 4000 m vertical section, and geothermal gradient of 33 °C km^{-1}. A three-dimensional geological domain surrounded the DCHE geometry that extended sufficiently away from both planarly and vertically from the borehole closed-loop to prevent boundary effects. Harris et al., 2021 [6] ignore the impact of temperature and pressure and consider water to have constant properties. In addition to the code-to-code analysis previously stated, Ramey [57] analytical solution is used to validate the numerical model. Ramey's solution accounts for injecting cold fluid into a linear pipe encircled by rocks with temperatures escalating at greater depths. Beside the simple Stoke model, other more complex frictional resistance models [64–68] were tested. The results are shown in Table 2. We conduct a comparative assessment against our numerical results. Specifically, temperatures are assessed at the bottom of the injection well (R_1), and the wellhead of the producing well (H_1). The models were solved for 50 years [6]. Fig. 4 depicts the isothermal surfaces of the wellbore and formations within the model.

The fluid temperatures along the system's length at different times are displayed in Fig. 5a. The fluid gains thermal energy as it descends the first well because the ground temperature rises with depth, which is at the end of the vertical section 4000 m. The fluid experiences the most tremendous temperature increase in the horizontal segment, which is 4800 m, since it has the system's highest ground temperature. The fluid's temperature rises and reaches a maximum as it ascends the production well, but it then begins to lose some heat toward the earth's surface. The fluid temperature stabilises over time, exhibiting progressively smaller changes with each successive decade. The observed settling trend is further elucidated by examining the outlet temperature as depicted in Fig. 5b. The fluid exhibit same behaviour in Ramey solution [57], and Harris et al.'s [6] solution as can be observe in Fig. 5b, initially, during the commencement of operations, there is a swift decline in the outlet temperature, succeeded by gradual and comparatively minor decreases over extended periods.

Although the Stoke frictional resistance model doesn't account for the borehole roughness (ε, mm), the solutions adopting this simple frictional resistance model agree with the cited models within the allowable ±3% percentage error. We concluded that the combination of parameters that yields this outcome strikes a good balance between

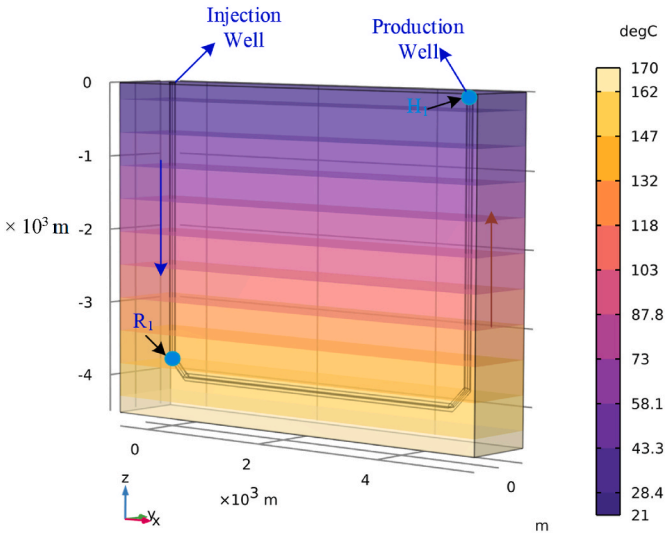

Fig. 4. Isothermal profiles of the near well strata and the wellbore after fifty years of continuous production.

Table 2
Comparison of production temperature (at the 50th year) adopting different frictional resistance models, at the bottom of the injection Ramey's [57], and top of the production well Harris et al. [6] solution.

Models	Frictional resistance models output temperatures (°C)					
	Holland [64]	Churchill [65]	*Stokes [53]	Wood [66]	Colebrook [67]	Swamee-Jain [68]
Ramsey's result [57] (38.5 °C)	37.14	37.01	37.19	37.13	37.14	37.16
Harris et al. [6] (73 °C)	77.55	77.57	75.17	77.55	77.50	77.58
Error Ramey's solution.	−1.36	−1.49	−1.31	−1.37	−1.36	−1.34
Error Harris et al. solution	+4.55	+4.57	+2.17	+4.55	+4.50	+4.58

Note: Stokes model was adopted due to its high accuracy compared to other frictional resistance models.

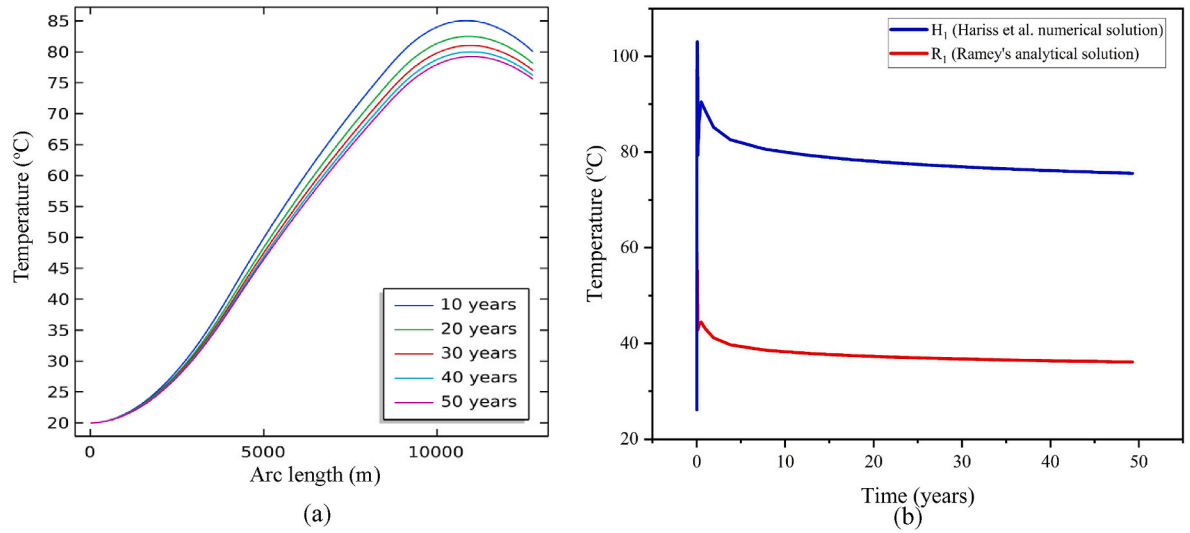

Fig. 5. Comparison of the fluid temperature along the base case system's length 10–50 years with Harris et al. [6] (a); Comparison of output temperatures from stokes model at the production well against Harris et al. [6], and bottom of the injection well against Ramey's solution [57] after 50 years of continuous production (b). The computation results adopting different frictional resistance models are displayed (see Table 2).

computation time and the necessary accuracy. Therefore, the mesh, frictional resistance model, and relative tolerance settings were maintained during this study.

4. The DCHE benchmark model

The goal of this research is to identify the best long-time production time-dependent operation of triplet deep borehole heat exchanger for maximum recovered thermal energy. We design based on long-time production of 25 years of heat extraction. The following materials were considered for both casing and tubing: the thickness of the concrete casing (r_c -r_b) is 20 mm, and the vertical, horizontal and deviated sections all have 150 mm borehole inner diameters (D), thermal conductivity (λ), and roughness (ε) Table 3 lists the materials used in the simulation for well completion. The average density, heat capacity, and thermal conductivity of the isotropic and homogeneous geological formation in which the DCHE is embedded are 2450 kgm^{-3}, 964 ($Jkg^{-1}K^{-1}$), and 3.2 ($Wm^{-1}K^{-1}$), respectively. With a surface temperature of 27 °C, the temperature below rises with depth in accordance with a linear geothermal gradient (G_{geo}) of 31 °C km^{-1}. The primary fluid was injected into the two injection wells with a circulation (q_v) of 0.004 $m^3 s^{-1}$ (4 kg s^{-1}). The rationale is that as the fluid converges at the production well's bottom, the flow rate increases to 0.008 m^3s^{-1}, which ultimately reduce the loss of heat at the production well, with an initial temperature of injection (T_{inj}) of 20 °C. As depicted in Fig. 6, the fluid expeditiously initiated heat exchange with the surrounding rocks upon commencement of circulation. This thermal interaction led to the fluid

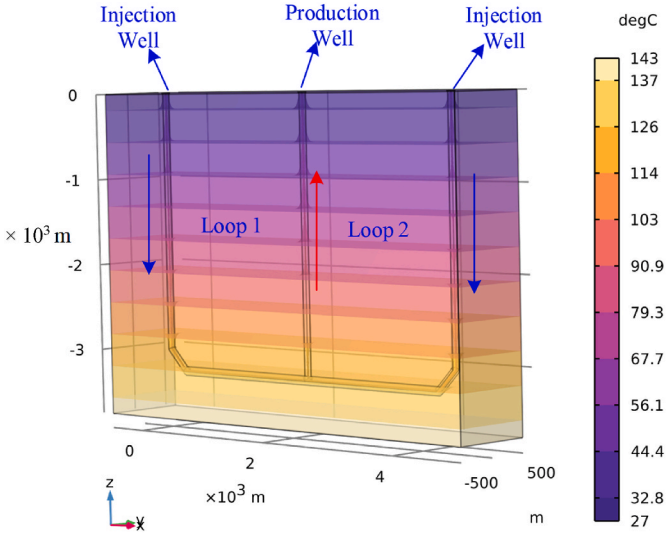

Fig. 6. Isothermal contours profiles of the near well strata and wellbore after 25 years of continuous production.

achieving a temperature surpassing its initial injection temperature upon reaching the production wellhead. Subsequently, the fluid underwent a heat exchange process with the geothermal plant through a working fluid in a dedicated heat exchanger. Determining the precise

Table 3
Materials employed in well completion and the encompassing geological formations have different properties. Non-thermal enhanced concrete (NTHC), Thermally enhanced concrete (THC). Lyons et al., 2020 [69][aa]; Allen 1996 [70][bb]; Mascarin et al., 2022 [71][cc]; Renaud et al., 2021 [72] [dd]; Pan et al., 2020 [73] [ee].

Properties	Expression	Materials for borehole completion				Surrounding rock
		Concrete casing		Tubing		
		NTHC	THC	Steel	Polyethylene	
Absolute Roughness (mm)	ε	6[aa]	6[aa]	0.0457[bb]	0.0015[bb]	–
Wall thickness (mm)	d	20	20	9	9	–
Thermal conductivity ($Wm^{-1}K^{-1}$)	λ	1.5[cc]	2.5[cc]	45[dd]	0.50[ee]	3.2
Density (kgm^{-3})	ρ		–	–	–	2450
Heat capacity ($Jkg^{-1}K^{-1}$)	cp		–	–	–	964
Pipe diameter (mm)	D	–	–	150	150	–

Note: NTHC represents non-thermally enhanced concrete, and THC represents thermally enhanced concrete.

temperature requisite for the intended application informed the subsequent reduction in the primary fluid's temperature, denoted as $\Delta T = 20\ ^{\circ}C$. The insulated pipeline allowed the fluid to return to the two injection wells without losing heat to the surroundings. The injection temperature varied per Eq. (10) for operating times greater than zero. In areas in which the temperature of the fluid at the surface exceeded the subsurface one, the fluid cooled by releasing heat to the nearby rocks. These approximately occur at a well's length of roughly 520–950 m, the injection (downward) and extraction (upward) boreholes experienced the cooling effect.

The entire amount of time the fluid particle has been inside the borehole is known as its residence time. It has an inverse relationship with fluid velocity and a direct relationship with the two closed-loop lengths. As time passed, the liquid temperature profile changed in Fig. 7a and b. The temperature fluctuations were substantial initially, but temperature regimes demonstrated a nearly steady-state behaviour over longer functioning times after a while. After about 24 h, the production temperature for the benchmark model setting rose quickly to 67 °C, and after 90 days of operation, it reached a peak of 97 °C. The production temperature then started to drop gradually. The DCHE sustain a fluid output temperature of roughly 91 °C over twenty-five years of the operating period under investigation, as shown in Fig. 7b.

5. Parametric study on total recovered thermal energy of DCHE

To investigate the impact of the optimal periodic design on the energy efficiency of the DCHE, we ran a series of heuristic simulations in which we varied the operating design. Our benchmark model parameters, such as the rock's thermal properties and the undisturbed geothermal gradient (G_{geo}), remain unchanged. The variables governing the operation include the thermal energy extracted from the heat-exchanging primary fluid (ΔT), or equivalently, the temperature of injection (T_{inj}), in conjunction with the circulation rate (q_v). For the sensitivity analysis, we selected our benchmark model's electrical power generated (TWe) as the parameter for the model response. The results of our parametric study are shown in Table 4, and the output temperature is shown in Fig. 8a and b. Based on our parametric studies, switching between loop one and loop two can be a good compromise, demonstrating total recovered thermal energy and the electrical power generated by the periodic interchange of loop one and two is on the increasing pattern, unlike the other investigations.

5.1. Operating variables

The two closed-loop systems can operate sustainably, characterised by economically viable circulation rates and production temperatures, by ensuring a balance between subsurface heat extraction and subsequent thermal energy recovery. The fluid circulation around the borehole causes a noticeable cooling effect during the 365 days a year, 24 h a day that the system is in operation, as observed in the benchmark model Fig (7a, and b) which resulted in recovering total thermal energy of 1897 TW_{th} over 9000 days (25 years) of nonstop production, with an injections rate of (0.004x2 m^3s^{-1}), the production temperature shows a declining pattern as can be observed in Fig. 7b. While for the periodic production on six monthly bases, the system generates total recovered thermal energy of 1059 TW_{th} over 9000 days (25 years) of production, with an injection rate of (0.004x2 m^3s^{-1}), the production temperature maintained the same output pattern throughout investigation as shown in Fig. 8a (blue zigzag line), take note: the system operates for only 12.5 years, and 12.5 years of energy recovery. While the periodic interchange of loops one and two on six monthly basis the system generates total recovered thermal energy of 880 TW_{th}, with an injection rate of (0.004 m^3s^{-1}), the production temperature shows an increasing pattern, as can be observed in Fig. 8b. The periodic production by interchanging loop one and two by six monthly basis presents better results based on the pattern of increasing production temperature, as the aim of the research is to identify the best long-term operation design for total recovered thermal energy and heat recovery without interruption in production.

The operational variables are critical parameters influencing the energy recovery Eq. (14) and exerting substantial influence on the DCHE long-term thermal performance (q_v and ΔT). Focusing on circulation rate and employing relatively low q_v values within the range of 0.003–0.015 m^3s^{-1}, previous coaxial numerical simulations yielded promising outcomes in terms of thermal performance and sustainability [36,72,74]. But for direct heat applications, the average circulation rate of economically viable applications ought to be between 0.030 and 0.100 $m^3\ s^{-1}$ [75] and between 0.030 and 0.200 m^3s^{-1} to produce electricity [61]. Take note: multiple wells operating in a production field are the only way to achieve the highest circulation rates listed here. We decided to use 0.03 m^3s^{-1} as our injection rate for our case study, which is a good compromise for both direct usage and power generation. We also adopted the best operating design learned from our parametric analysis, we adopt switching production between close loop one and close loop two on a six-monthly basis, which offers a good compromise

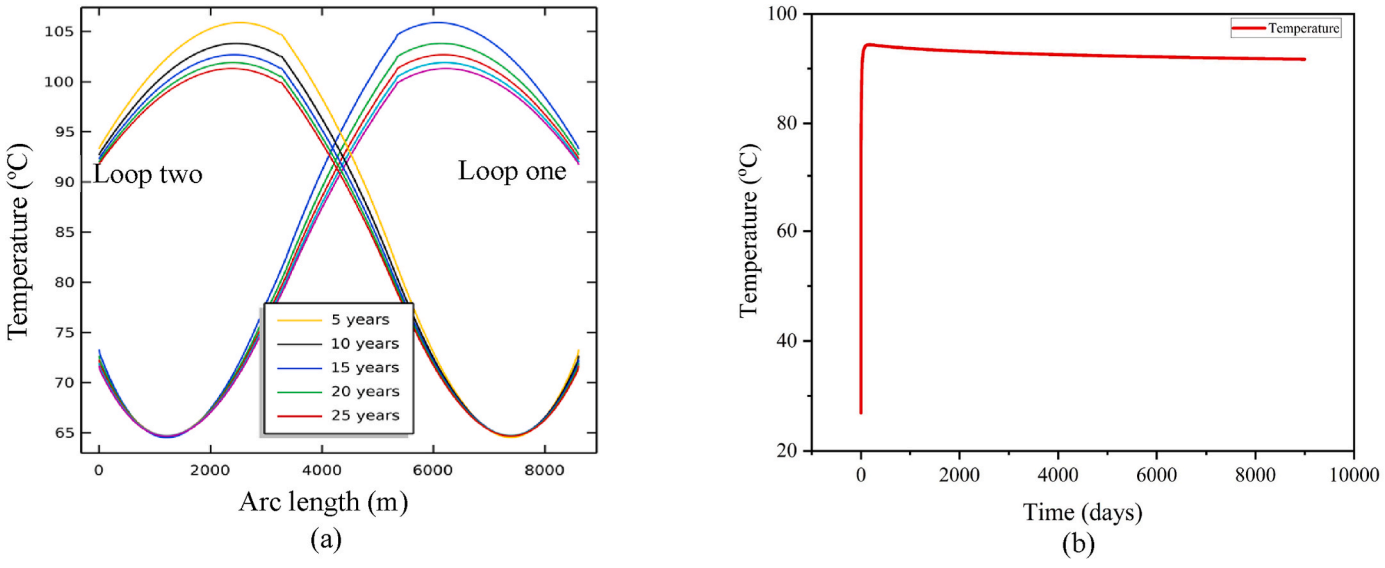

Fig. 7. Benchmark model (DCHE) Fluid temperature along the base case system's length 5–25 years of continuous production (9000 days) (a); Benchmark model (DCHE) Output temperature after 25 years (9000 days) of continuous production (b).

Table 4
Parametric investigation on the DCHE models' operational changes, production temperature, average thermal power, total recovered thermal energy, and electrical power generated. T_{inj} 20 °C, ΔT is the fixed temperature of injection, which changes over time by equation (13).

Model	Variables						T_{prod}(°C) after 25 years	Av. Thermal power	Total. recovered thermal energy	Electrical power generated
	Environmental	Design				Operating				
	G_{geo}(°C km^{-1})	H (km)	L(km)	D (m)	Materials	q_v (m^3s^{-1})	°C	MW_{th}	TW_{th}	TWe
Benchmark model	31	3	4 (2x2)	0.15	$STL_{inj.}$ $CON_{lat.}$ $PE_{prod.}$	0.004x2	91	2.33	1897	122
Periodic (six monthly basis)	31	3	4 (2x2)	0.15	$STL_{inj.}$ $CON_{lat.}$ $PE_{prod.}$	0.004x2	94	2.50	1060	64
Interchange (loop 1 and 2 by six months)	31	3	2x2	0.15	$STL_{inj.}$ CON_{lat} $PE_{prod.}$	0.004	88	1.10	880	53

Notes: The temperature here coincides with 9000 days (25 years). (STL, steel: PE, Polyethylene: CON, Concrete).

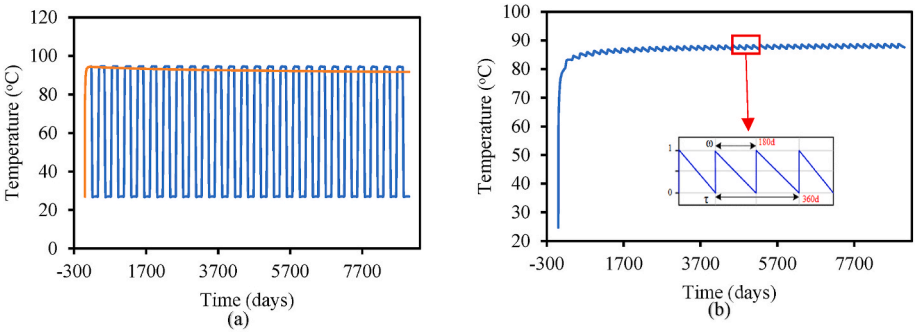

Fig. 8. Temperature variations with time in a periodic production (Blue Zigzag line on a six-monthly basis) compared to continuous operation (orange straight line) over 9000 days (25 years) (a); Production temperature by interchanging production from loops one and two, adopting a six-monthly basis over 9000 days (25 years) of production (b). (For interpretation of the references to colour in this figure legend, the reader is referred to the Web version of this article.)

for total recovered thermal energy without interruption in production, as shown in Fig. 8b.

5.2. Design variables

The most important design elements were the closed-loop dimensions. The maximum available depth was directly related to the heat carrier fluid's maximum temperature below ground. As shown in our benchmark model Fig. 6, which is in direct relationship with the geothermal gradient, the vertical length of our benchmark model is 3 km, which gives 91 °C, as the temperature of production over 25 years of continuous production. However, the output temperature will be higher if the horizontal length (L) is increased [76]. The observed phenomenon is anticipated, given that parameter L alterations will definitely impact the fluid circulation length, thereby influencing residence and heating durations. Consistent with our benchmark model, we maintain uniform thermal conductivity and roughness properties for well-completion materials, encompassing tubing and backfilling concrete. Due to its direct relationship to the fluid-rock formation contact surface and, consequently, to the radial heat transfer Eq. (8), the diameter and completion materials were also maintained as our benchmark model.

5.3. Geothermal gradient of the study area

The thermal performance of deep borehole heat exchangers is notably impacted by underground thermal conditions (G_{geo}) [33], the geothermal gradient is a crucial parameter in geothermal energy exploration and utilisation. It represents the rate of increase in temperature with depth beneath the earth's surface. Understanding the geothermal gradient is essential for assessing the heat potential in subsurface layers, guiding the design of geothermal systems, and optimising thermal energy extraction for sustainable and efficient geothermal power generation.

Scholars like [42,77,78] reported closely aligned estimates for the geothermal gradient within the Chad Basin, Nigeria, utilising corrected bottom hole temperature (BHT) data, and modified centroid method. They reported values ranging from 30 to 45.9 °C km^{-1}. Table 5 presents the values reported for our wells of interest. We take the average values of the three wells for the geothermal gradient for our simulation, which is approximately 37 °C km^{-1} for the three wells.

6. Study area

We systematically incorporated technical profiles of boreholes, geological and geothermal data, and ideal operating parameters from the preceding parametric sensitivity study to assess the feasibility of a two-loop combined system (DCHE). Stratigraphic data from designated wells Fig. 1 informed site-specific 3D geological models Fig. 9. We determined the lithologies' specific heat, density, and rock thermal conductivity through extensive bibliographic collections [51,46]. The intricate numerical models also include thermal conductivities and surface roughness of borehole completion materials for casing and

Table 5
Reported geothermal gradients in °C km^{-1} of GUB, NGA, and NGO from corrected BHT data, and modified centroid method.

Well	[42]	[77]	[78]	Average
GUB	33.2	NA	NA	33.2
NGA	38.7	42.9	40	40.5
NGO	38.7	NA	34	36.4

NA: (Not available).

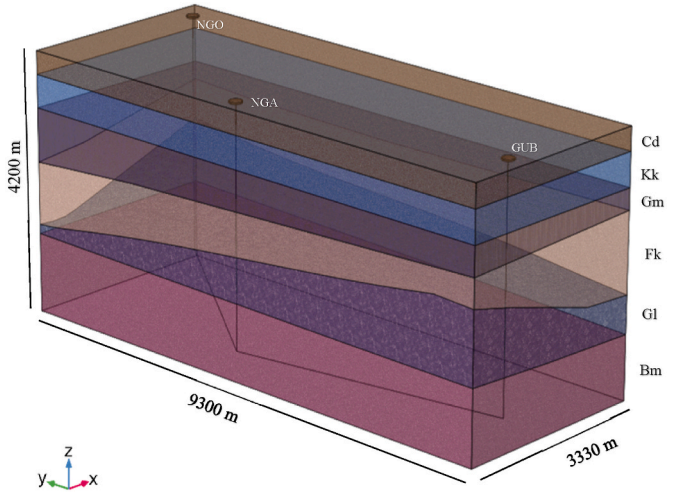

Fig. 9. 3D representation of the geological model configuration contained within the geological domain, along with the DCHE numerical models. The litho-thermal formations' code and numerical domain dimensions.

tubing.

6.1. Nigerian sector of the Chad Basin setting

The creation of two close loops system (DCHE) involves three deep abandoned petroleum wells which utilise the actual data and locations of the abandoned wells with similar profiles, with inner diameters of 150 mm from the surface to the bottom at 4000 m (bgl). In theory, the geothermal conditions in this setting are favourable for generating heat and electrical power [43,79].

We employed a rate of circulation of 0.030 m^3s^{-1} to examine the feasibility of such an application [75], which falls within the range of mostly adopted in deep heat exchangers and injection temperatures, which varies according to Eq. (10). The initial concept of connecting three boreholes via lateral leg, thereby creating two different loop cycle with three deep wells making it a unique or one-of-a-kind system is to ensures a steady uninterrupted production by six-monthly rotation between loop one and loop two. The operating configuration consists of twelve and half year's cycles each over the entire 25-years simulated time. Each loop thus functions for six months, with an additional rest period of six months to promote thermal recovery. Based on the design, the two opposite boreholes serve as the injection wells, while the middle borehole serves as the production well that serves the two loops. We also consider insulation material: the borehole casing is made with concrete (THC), for the injection wells, and the horizontal section, while the production well casing is made of concrete (NTHC), while the tubing are made with high conductive material (steel) for the injection wells, the horizontal tubing is made with concrete (THC), and the production well is made with low conductive material (polyethene), that has thermal conductivities and surface roughness (see Table 3).

The isothermal surfaces of temperature distribution within the wells and surrounding formation are shown in Fig. 10. The first loop gives an output temperature of 121.3 °C at day 180, production temperature attains its peak at day 181, which coincides with day one (1) of the second loop, which gives 135.5 °C. The loop ended with a temperature of 123 °C at day 360, the system sustained an output temperature of 113 °C over 9000 days (25 years) of interchangeable operation. The periodic interchangeable production temperature is presented in Fig. 11, which gives total recovered thermal energy and electrical power generated as 9730 TW_{th} and 817 TW_e using Eqs. (14) and (16) over twenty-five years (9000 days) of production, with an average of 389 TW_{th} and 33 MW_e per year, respectively.

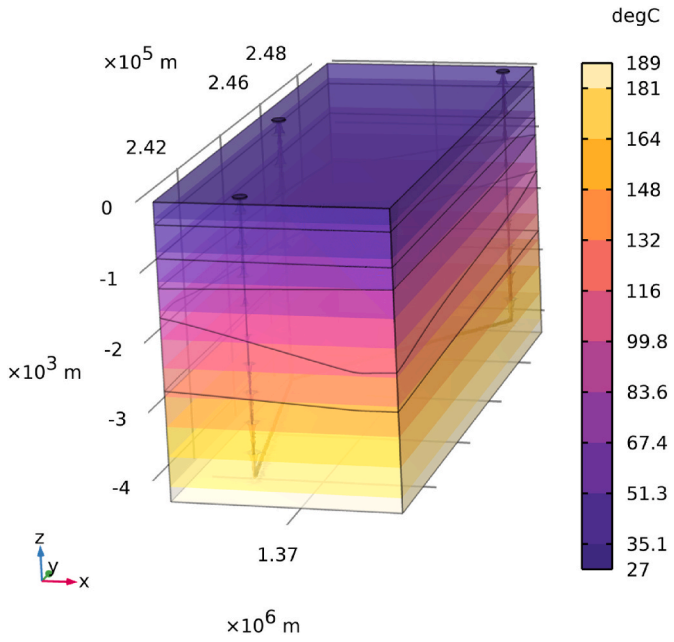

Fig. 10. Isothermal contours and coordinate system (UTM) of the loops contained within the 3D geological model after 25 years (9000 days) of interchangeable production.

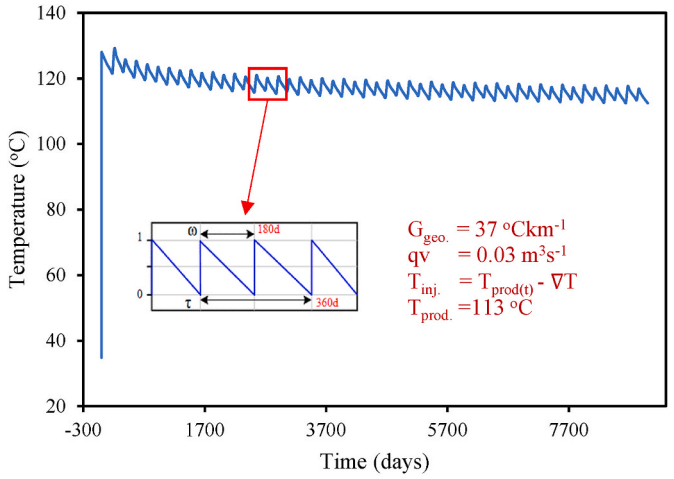

Fig. 11. Time depended production temperature by interchanging loop one and loop two by six monthly basis over 25 years (9000 days) of operation.

7. Results

To confirm the feasibility of DCHE for extended energy production from the site, which is characterised by intermediate temperature, we opted for 0.03 m^3s^{-1} circulation rates in our simulation. The value falls within the range (0.03–1 m^3s^{-1}) typically used in most deep geothermal applications, which is greater than the range 0.003–0.015 m^3s^{-1}, primarily adopted in coaxial deep borehole heat exchanger models. we decided to simulate the systems for a comparatively long period to observe the system's long-term performance. Furthermore, previous numerical simulations of deep borehole heat exchangers revealed that long-term performance can be studied in 25 years of heat extraction [80].

Additionally, we observed in our simulation that the water temperature increases rapidly, then drops, and later exhibits gradual reduction. This phenomenon is caused by the radial cooling from the borehole-rock interface gradually expanding its influence area. Following this transient

phase, the water temperature exhibits a linear decrease over time, albeit at a reduced rate, approaching negligibility. In our perspective, numerical models that account for time-dependent variations over twenty-five years yield crucial data for conducting a comprehensive long-term performance analysis.

The heat extraction rate from the wells, as illustrated in Fig. 12a, exhibits a comparable trend to the outlet temperature. At the onset of operation, there is an initial rise in the heat extraction rate, followed by a subsequent decline in later stages. The temperature and heat extraction outcomes exhibit a consistent correlation. Throughout 25 years, the heat extraction rate has consistently stayed above 30 TW, signifying a substantial amount of thermal energy. This valuable resource holds the potential for various heating/electricity production.

Fig. 12b, illustrates theoretical power generated, and from binary cycle with relative efficiency of 58% for power production. The curves exhibit similarity from the onset of production to the end, after 9000 days (25 years) of production we obtained 1401, and 817 TWe from theoretical, and binary cycle with relative efficiency of 58% respectively. After 9000 days (25 years) of interchangeable operation, a binary cycle with 58% relative efficiency yield approximately 2.44 TWe, resulting in a total electrical energy generation of 817 TWe over the entire operational period. This valuable resource can be integrated to the dilapidated power sector of Nigeria.

The erratic electricity supply has emerged as a critical issue significantly impeding Nigeria's economic development. For an initial evaluation of the (DCHE) systems to fulfil energy requirements, we established the energy requisites for typical energy demand per capita in the north-eastern part of Nigeria. The requirements for energy demand are summarise as follows.

- In 2015, per capita annual electricity consumption was 140 kWh, or about 12 kWh per month, according to the IEA [81].
- The monthly energy consumption of urban dwellers is 39 kWh per capita, while that of rural residents is 17 kWh per capita. North East had the lowest monthly per capita electricity consumption (about 1 kWh per capita) [82].
- The daily electrical consumption of urban hospital is 343.23 kWh/day, which stand as 123562.8 kW/year [83].

The above data was used in our computations, with the generated energies obtained from our study which stand as follows.

- The total recovered thermal energy is 9730 $TW_{th,}$ averaging 389 TW_{th} annually.
- The total electricity generated over 9000 days (25 years) of production is 817 $TW_{e,}$ an average of 33 TW_e per year.

According to Ref. [84], the population of the Magumeri district is projected to be 205,500, with an average electricity consumption of 1 kW_{th} (0.03 per day) per capita [81]. The 33 TWe electricity generated annually is more than enough for the entire population together with hospital electricity need. The excess of approximately 89,267,120 kWh of electricity available daily from the geothermal binary plant can sustain the geothermal binary plant operation considering efficiently sized pump systems consume 0.9 kW per kg of geothermal fluid pumped with average consumption of 1.25 kW/kg, when considering flow rate of 60 kg s^{-1}, the required pumping power should be between 55 and 75 kW. The excess electricity generated by our geothermal binary plant can indeed be converted into direct usage for applications such as district heating and cooling. Considering a conversion efficiency of about 70% for converting this electricity into thermal energy for heating or cooling, this results in a potential thermal energy availability of approximately 62,487,127 kWh per day. This substantial amount of thermal energy could be used to provide district heating or cooling. This investigation unequivocally demonstrates that the suggested DCHE system concepts would allow technology to extract geothermal energy effectively to meet the needs for electricity utilisation for our case study and thermal recovery simultaneously.

8. Conclusions

This research marks a significant advancement in geothermal energy utilisation by introducing a pioneering (DCHE) two closed-loop system, utilising three abundant wells that seamlessly integrate heat production and thermal recovery without any interruptions in the production process. The creation of two distinct loops represents a novel approach, leveraging abandoned petroleum wells in the Nigerian sector of the Chad Basin as a sustainable and uninterrupted source for geothermal power generation.

A comprehensive understanding of the geothermal and heat flow characteristics of the selected wells drove the development and optimisation of these dual loops. The use of advanced simulation tools, particularly COMSOL Multiphysics, played a pivotal role in achieving an optimal operating design by conducting a parametric study on the best operation design in terms of total recovered thermal energy and electricity production that carter for heat recovery at the same time without interruption in production. We also explored insulating the production well pipes entering and exiting the geothermal plant to minimise energy loss. We also insulate the injection wells using high-conductive materials to optimise heat energy exchange between the fluid and the surrounding rocks. We also considered the thermal conductivity and surface roughness of the borehole completion materials. In our study, we contribute to understanding long-term functionality and the optimal operation design of DCHE systems. We conclude as follows:

- Periodic interchange of loops one and two is recommended when there are more than two wells available. Continuous production significantly affects the two-loop system, which can lead to thermal breakthroughs. In contrast, periodic production on six monthly basis maintains the same output temperature from the beginning to the

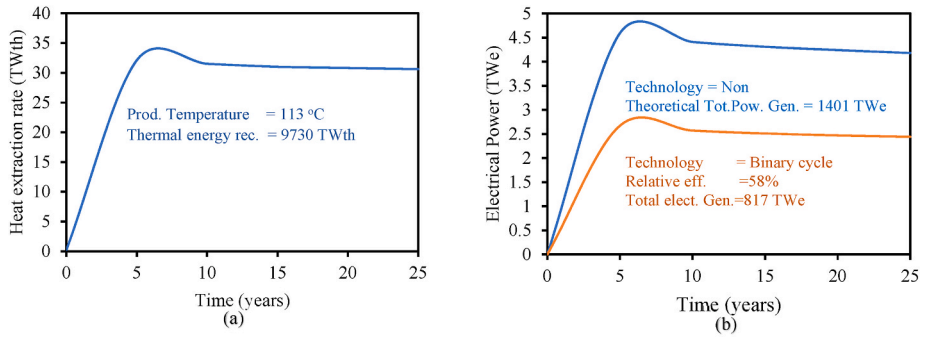

Fig. 12. Heat extraction from the outlet fluid over 25 years of investigation (a); Theoretical electrical power generated, and power generated with a binary cycle with relative efficiency of 58% over 9000 days (25 years) of investigation (b).

end of the investigations but with alternating production and heat recovery.

- A medium injection flow rate is recommended when there are more than two deep boreholes with a lateral distance of more than 4000 m in an intermediate temperature resource to generate electricity. This study considers the injection rate of 0.03 m^3s^{-1} with varying injection temperatures.
- The DCHE systems sustain electrical power production by binary plants. In our test site, we generated thermal and electrical power of 9730 TW_{th} and 817 $TW_{e,}$ respectively, which is more than enough for the entire population of Magumeri district. We are anticipating a plant that can guaranty sustainable power not only for Magumeri district along, but also with neighbouring districts

This research established two distinct loop systems from three abandoned wells with the following advantages. Firstly, two injections converge to give a double flow rate, which will ultimately increase the speed of the fluid to minimise loss of heat at the production. Secondly, the loops can operate independently or simultaneously without interruption in production. Thirdly, as demonstrated in our study, it can be used in intermediate to high geothermal fields to generate thermal and electrical energy without interruption. Fourthly, it can recover its thermal energy while the system is still operating. Finally, sensitivity studies for the best operating design were developed.

In contrast to a single loop system, this novel configuration of two deep close loop heat exchangers (DCHE) reasonably augments the overall length designated for heat exchange. Moreover, it improves fluid residence time and long-term thermal performance, thereby mitigating the occurrence of detrimental thermal breakthrough between the inflow and outflow of the heat carrier fluid circulation. The potential for cyclic production in deep borehole exchange systems, characterised by interchanging operation between the loops, represents a sustainable practice from energy, functional, and environmental perspectives.

Relevant parameters, including thermal properties of the lithologies, thermal conductivities, and surface roughness of the insulation materials, are considered. Still, work needs to be done to integrate the heterogeneity of the abandoned well's reservoir in the numerical simulation to enhance the numerical model.

Data availability

Data will be provided on request.

Nomenclature

NNPC	Nigerian National Petroleum Corporation
IEA	International Energy Agency
NAPIMS	Nigerian National Petroleum Investment Management Service
UTM	Universal Transverse Mercator
TVD	True Vertical Depth
NTHC	Non-Thermally Enhanced Concrete
THC	Thermally Enhanced Concrete
DBHE	Deep borehole heat exchanger
DCHE	Deep close loop heat exchanger
BHT	Bottom hole temperature
NA	Not Available
Gl	Gongila
PE	Polyethylene
fD	Frictional resistance factor
t	Time (s)
λn	Thermal conductivity of rock (Wm-1K-1)
F	Gravity volume force (Nm-3)
ρc	Volumetric heat capacity (J m-3 K-1).
Cρn	Specific heat capacity rock (J/(kg·K))
Gth	Thermal power (MWth)
Ge	Electrical power (TWe)
T(z,t)	Fluid temperature in the wellbore (K)
Cρm	Specific heat capacity of water (J/(kg·K))
λm	Thermal conductivity of the fluid (Wm-1K-1)
D	Borehole inner diameter (m)
ρm	Fluid density (kgm-3)
GUB	Gubio
NGO	Ngor
Fm	Formation
NGA	Ngamma
F(t)	Transient heat transfer
Cd	Chad
Kk	Kerri kerri
Gm	Gombe
Fk	Fika
Bm	Bima
STL	Steel
CON	Concrete
Y	Depth of temperature measurement (m)
P	Pressure (Pa)
A	Cross-section area (m2)
ρn	Density of rock (kgm-3)
ηideal	Ideal thermal performance
qv	Volumetric flow rate (m3s-1)
ηrel	Relative efficiency
rw	Well radius (m)
α	Thermal diffusivity (m2s-1)
Qw	Heat source (W m-1)

CRediT authorship contribution statement

Abubakar Magaji: Data curation, Investigation, Writing – original draft, Conceptualization, Methodology. **Bin Dou:** Data curation, Investigation, Writing – original draft, Supervision. **Gianluca Gola:** Conceptualization, Data curation, Validation, Writing – review & editing, Methodology. **Sani Ali:** Investigation, Writing – original draft. **Ibrahim AL-Wesabi:** Visualization.

Declaration of competing interest

The authors declare that they have no known competing financial interests or personal relationships that could have appeared to influence the work reported in this paper.

Acknowledgments

This research was supported by The National Key Research and Development Programs of Henan Province, grant number 231111320800; The Open Fund of Shanghai Shallow Geothermal Energy Engineering Technology Center, grant number DRZX-202303.

References

[1] Siddiqui O, Ishaq H. A geothermal energy driven integrated energy system for fresh water and power production. Int J Hydrogen Energy 2023;48:39032–42.
[2] Yuksel YE, Ozturk M. Thermodynamic and thermoeconomic analyses of a geothermal energy based integrated system for hydrogen production. Int J Hydrogen Energy 2017;42:2530–46.
[3] Ramazankhani M-E, Mostafaeipour A, Hosseininasab H, Fakhrzad M-B. Feasibility of geothermal power assisted hydrogen production in Iran. Int J Hydrogen Energy 2016;41:18351–69.
[4] Prieto MP, Solomakhina N, de Uribarri PMÁ. Multimodal networks and decentralized renewable generation: network modeling and energy/exergy performance evaluation. Urban energy syst. Low-carbon cities. Elsevier; 2019. p. 181–239.
[5] Vivas C, Salehi S, Tuttle JD, Rickard B. Challenges and opportunities of geothermal drilling for renewable energy generation. GRC Trans 2020;44:904–18.
[6] Harris BE, Lightstone MF, Reitsma S. A numerical investigation into the use of directionally drilled wells for the extraction of geothermal energy from abandoned oil and gas wells. Geothermics 2021;90:101994.
[7] Bu X, Ma W, Li H. Geothermal energy production utilizing abandoned oil and gas wells. Renew Energy 2012;41:80–5.
[8] Lund JW, Toth AN. Direct utilization of geothermal energy 2020 worldwide review. Geothermics 2021;90:101915.
[9] Zhu Y, Li K, Liu C, Mgijimi MB. Geothermal power production from abandoned oil reservoirs using in situ combustion technology. Energies 2019;12:4476.

[10] Caulk RA, Graduate MS, Tomac I. Reuse of abandoned oil and gas wells for geothermal energy production. Renew Energy 2017;112:388–97. https://doi.org/10.1016/j.renene.2017.05.042.
[11] Sapinska-Sliwa A, Rosen MA, Gonet A, Sliwa T. Deep borehole heat exchangers—a conceptual and comparative review. Int J Air-Conditioning Refrig 2016;24:1630001.
[12] Wight NM, Bennett NS. Geothermal energy from abandoned oil and gas wells using water in combination with a closed wellbore. Appl Therm Eng 2015;89:908–15.
[13] Noorollahi Y, Taghipoor S, Sajadi B. Geothermal sea water desalination system (GSWDS) using abandoned oil/gas wells. Geothermics 2017;67:66–75.
[14] Ogbuigwe A. Refining in Nigeria: history, challenges and prospects. Appl Petrochemical Res 2018;8:181–92.
[15] Bull AS, Love MS. Worldwide oil and gas platform decommissioning: a review of practices and reefing options. Ocean Coast Manag 2019;168:274–306.
[16] Chen C, Cai W, Naumov D, Tu K, Zhou H, Zhang Y, et al. Numerical investigation on the capacity and efficiency of a deep enhanced U-tube borehole heat exchanger system for building heating. Renew Energy 2021;169:557–72.
[17] Weijermars R, Burnett D, Claridge D, Noynaert S, Pate M, Westphal D, et al. Redeveloping depleted hydrocarbon wells in an enhanced geothermal system (EGS) for a university campus: progress report of a real-asset-based feasibility study. Energy Strategy Rev 2018;21:191–203.
[18] Stefani E, Muñoz M, Morata D, Rojas L, Rioseco EM. Rehabilitation of petroleum wells as borehole heat exchangers to provide heat for district heating networks in small towns or villages: case study in magallanes basin. Artículo En Prep 2018:1–9.
[19] Sun X, Wang Z, Liao Y, Sun B, Gao Y. Geothermal energy production utilizing a U-shaped well in combination with supercritical CO2 circulation. Appl Therm Eng 2019;151:523–35.
[20] Kaplanoğlu MA, Baba A, Gokcen Akkurt G. Use of abandoned oil wells in geothermal systems in Turkey. Geomech Geophys Geo-Energy Geo-Resources 2020;6:1–10.
[21] Sui D, Wiktorski E, Røksland M, Basmoen TA. Review and investigations on geothermal energy extraction from abandoned petroleum wells. J Pet Explor Prod Technol 2019;9:1135–47.
[22] Wang K, Yuan B, Ji G, Wu X. A comprehensive review of geothermal energy extraction and utilization in oilfields. J Pet Sci Eng 2018;168:465–77.
[23] Śliwa T, Kruszewski M, Assadi M, Sapińska-Śliwa A. The application of vacuum insulated tubing in deep borehole heat exchangers. AGH Drilling, Oil, Gas 2017;34.
[24] Boothroyd IM, Almond S, Qassim SM, Worrall F, Davies RJ. Fugitive emissions of methane from abandoned, decommissioned oil and gas wells. Sci Total Environ 2016;547:461–9.
[25] Kang M, Kanno CM, Reid MC, Zhang X, Mauzerall DL, Celia MA, et al. Direct measurements of methane emissions from abandoned oil and gas wells in Pennsylvania. Proc Natl Acad Sci USA 2014;111:18173–7.
[26] Kohl T, Salton M, Rybach L. Data analysis of the deep borehole heat exchanger plant Weissbad (Switzerland). Proc. world Geotherm. Congr.; 2000. p. 3459–64.
[27] Kohl T, Brenni R, Eugster W. System performance of a deep borehole heat exchanger. Geothermics 2002;31:687–708.
[28] Hu X, Banks J, Guo Y, Liu WV. Retrofitting abandoned petroleum wells as doublet deep borehole heat exchangers for geothermal energy production—a numerical investigation. Renew Energy 2021;176:115–34.
[29] Liao Y, Sun X, Sun B, Wang Z, Wang J, Wang X. Geothermal exploitation and electricity generation from multibranch U-shaped well–enhanced geothermal system. Renew Energy 2021;163:2178–89.
[30] Yuan W, Chen Z, Grasby SE, Little E. Closed-loop geothermal energy recovery from deep high enthalpy systems. Renew Energy 2021;177:976–91.
[31] Zhao Y, Ma Z, Pang Z. A fast simulation approach to the thermal recovery characteristics of deep borehole heat exchanger after heat extraction. Sustainability 2020;12:2021.
[32] Holmberg H, Acuña J, Næss E, Sønju OK. Thermal evaluation of coaxial deep borehole heat exchangers. Renew Energy 2016;97:65–76.
[33] Gola G, Di Sipio E, Facci M, Galgaro A, Manzella A. Geothermal deep closed-loop heat exchangers: a novel technical potential evaluation to answer the power and heat demands. Renew Energy 2022;198:1193–209. https://doi.org/10.1016/j.renene.2022.08.071.
[34] Szekszárdi A, Békési E, Tóth K, Sulyok I, Gáti M. WeHEAT SYSTEMS: a sustainable closed loop heating technology in the field of geothermal energy n.d.
[35] Kujawa T, Nowak W, Stachel AA. Utilization of existing deep geological wells for acquisitions of geothermal energy. Therm. Sci. 2004. Proc. ASME-ZSIS int. Therm. Sci. Semin. II. Begel House Inc.; 2004.
[36] Doran HR, Renaud T, Falcone G, Pan L, Verdin PG. Modelling an unconventional closed-loop deep borehole heat exchanger (DBHE): sensitivity analysis on the Newberry volcanic setting. Geoth Energy 2021;9:1–24.
[37] Alimonti C, Soldo E. Study of geothermal power generation from a very deep oil well with a wellbore heat exchanger. Renew Energy 2016;86:292–301.
[38] Adewumi T, Salako KA, Akingboye AS, Muztaza NM, Alhassan UD, Udensi EE. Reconstruction of the subsurface crustal and radiogenic heat models of the Bornu Basin, Nigeria, from multi-geophysical datasets: implications for hydrocarbon prospecting. Adv Space Res 2023;71:4072–90.
[39] Okosun EA. A preliminary assessment of the petroleum potentials from southwest Chad Basin (Nigeria). Borno J Geol 2000;2:40–50.
[40] Binks RM, Fairhead JD. A plate tectonic setting for Mesozoic rifts of West and Central Africa. Tectonophysics 1992;213:141–51.
[41] Obaje NG, Obaje NG. Petroleum resources. Geol Miner Resour Niger 2009:155–81.
[42] Awoyemi MO, Falade SC, Arogundade AB, Hammed OS, Ajama OD, Falade AH, et al. Magnetically inferred regional heat flow and geological structures in parts of Chad Basin, Nigeria and their implications for geothermal and hydrocarbon prospects. J Pet Sci Eng 2022;213:110388.
[43] Pollack HN, Hurter SJ, Johnson JR. Heat flow from the Earth's interior: analysis of the global data set. Rev Geophys 1993;31:267–80.
[44] Ali S, Orazulike DM. Well logs-derived radiogenic heat production in the sediments of the Chad Basin, NE Nigeria. J Appl Sci 2010;10:786–800.
[45] Emujakporue GO. Subsurface temperature distribution from heat flow conduction equation in part of Chad sedimentary basin, Nigeria. Egypt J Pet 2017;26:519–24.
[46] Ali SK, Onuaha M, Orazulike DM. Thermal diffusivity estimates in the Chad Basin, NE Nigeria-implications for petroleum exploration. ASSET An Int J (Series B)} 2012;3:155–71.
[47] Bata T, Parnell J, Samaila NK, Abubakar MB, Maigari AS. Geochemical evidence for a Cretaceous oil sand (Bima oil sand) in the Chad Basin, Nigeria. J Afr Earth Sci 2015;111:148–55.
[48] Omosanya KO, Akinmosin AA, Adio NA. The hydrocarbon potential of the Nigerian Chad Basin from wireline logs. Indian J Sci Technol 2011;4:1668–75.
[49] Adegoke AK, Sarki Yandoka BM, Abdullah WH, Akaegbobi IM. Molecular geochemical evaluation of Late Cretaceous sediments from Chad (Bornu) Basin, NE Nigeria: implications for paleodepositional conditions, source input and thermal maturation. Arabian J Geosci 2015;8:1591–609.
[50] Isyaku AA, Rust D, Teeuw R, Whitworth M. Integrated well log and 2-D seismic data interpretation to image the subsurface stratigraphy and structure in north-eastern Bornu (Chad) basin. J Afr Earth Sci 2016;121:1–15.
[51] Ali S, Orazulike DM. Estimation of the petrophysical parameters of sediments from Chad basin using well logs. Global J Geol Sci 2011;9:143–76.
[52] DiPippo R. Geothermal power plants: principles. Appl Case Stud Environ Impact 2008;2.
[53] Song S, Yang X, Xin F, Lu TJ. Modeling of surface roughness effects on Stokes flow in circular pipes. Phys Fluids 2018;30.
[54] Gnielinski V. New equations for heat and mass transfer in turbulent pipe and channel flow. Int Chem Eng 1976;16:359–67.
[55] Amestoy PR, Buttari A, L'excellent J-Y, Mary T. Performance and scalability of the block low-rank multifrontal factorization on multicore architectures. ACM Trans Math Software 2019;45:1–26.
[56] Yildirim N, Toksoy M, Gokcen G. Piping network design of geothermal district heating systems: case study for a university campus. Energy 2010;35:3256–62.
[57] Ramey Jr HJ. Wellbore heat transmission. J Petrol Technol 1962;14:427–35.
[58] Hagoort J. Ramey's wellbore heat transmission revisited. SPE J 2004;9:465–74.
[59] Satman A, Tureyen OI. Geothermal wellbore heat transmission: stabilization times for "static" and "transient" wellbore temperature profiles. Geothermics 2016;64:482–9.
[60] Moya D, Aldás C, Kaparaju P. Geothermal energy: power plant technology and direct heat applications. Renew Sustain Energy Rev 2018;94:889–901.
[61] Zarrouk SJ, Moon H. Efficiency of geothermal power plants: a worldwide review. Geothermics 2014;51:142–53.
[62] Bao J, Zhao L. A review of working fluid and expander selections for organic Rankine cycle. Renew Sustain Energy Rev 2013;24:325–42.
[63] DiPippo R. Ideal thermal efficiency for geothermal binary plants. Geothermics 2007;36:276–85.
[64] Haaland SE. Simple and explicit formulas for the friction factor in turbulent pipe flow. 1983.
[65] Churchill SW. Friction-factor equation spans all fluid-flow regimes. 1977.
[66] Wood DJ. An explicit friction factor relationship. Civ Eng 1966;36:60–1.
[67] Niazkar M. Revisiting the estimation of Colebrook friction factor: a comparison between artificial intelligence models and CW based explicit equations. KSCE J Civ Eng 2019;23(10):4311–26. 2019.
[68] Swamee PK, Jain AK. Explicit equations for pipe-flow problems. J Hydraul Div 1976;102:657–64.
[69] Lyons WC, Stanley JH, Sinisterra FJ, Weller T. Air and gas drilling manual: applications for oil, gas, geothermal fluid recovery wells, specialized construction boreholes, and the history and advent of the directional DTH. Gulf Professional Publishing; 2020.
[70] Allen RG. Relating the Hazen-Williams and Darcy-Weisbach friction loss equations for pressurized irrigation. Appl Eng Agric 1996;12:685–93.
[71] Mascarin L, Garbin E, Di Sipio E, Dalla Santa G, Bertermann D, Artioli G, et al. Selection of backfill grout for shallow geothermal systems: materials investigation and thermo-physical analysis. Construct Build Mater 2022;318:125832.
[72] Renaud T, Pan L, Doran H, Falcone G, Verdin PG. Numerical analysis of enhanced conductive deep borehole heat exchangers. Sustainability 2021;13:6918.
[73] Pan S, Kong Y, Chen C, Pang Z, Wang J. Optimization of the utilization of deep borehole heat exchangers. Geoth Energy 2020;8:1–20.
[74] Falcone G, Liu X, Okech RR, Seyidov F, Teodoriu C. Assessment of deep geothermal energy exploitation methods: the need for novel single-well solutions. Energy 2018;160:54–63.
[75] Lund JW, Falls K. Direct heat utilization of geothermal energy. Compr Renew Energy 2012;7:171–88.
[76] Düber S, Fuentes R, Narsilio GA. Comparison and integration of simulation models for horizontal connection pipes in geothermal bore fields. Geoth Energy 2023;11:15.
[77] Kwaya MY, Kurowska E, Arabi AS. Geothermal gradient and heat flow in the Nigeria sector of the Chad basin, Nigeria. Comput Water Energy Environ Eng 2016;5:70–8. https://doi.org/10.4236/cweee.2016.52007.
[78] John jitong shirputda. Assessment of geothermal resources in the Nigerian sector of the Chad basin, NE-Nigeria. 2019.
[79] Kappelmeyer O. Implications of heat flow studies for geothermal energy prospects. Terr. heat flow Eur. Springer; 1979. p. 126–35.

[80] Hu X, Banks J, Guo Y, Liu WV. Retrofitting abandoned petroleum wells as doublet deep borehole heat exchangers for geothermal energy production—a numerical investigation. Renew Energy 2021;176:115–34. https://doi.org/10.1016/j.renene.2021.05.061.
[81] Olaniyan K, McLellan BC, Ogata S, Tezuka T. Estimating residential electricity consumption in Nigeria to support energy transitions. Sustainability 2018;10:1440.
[82] Economic UND of I. World population prospects. UN; 1978.
[83] Nwanya SC, Ekechukwu OV. The energy performance of hospital buildings in Nigeria. Proc. Conf. Young Sci. Energy 2013:29–31.
[84] National Bereau for Statistic. Population projection for all LGAs within Nigeria. Web 2022. https://www.citypopulation.de/en/nigeria/admin/. The web page we accessed do not have volume number and page number.